GEOPHYSICS, VOL. 68, NO. 3 (MAY-JUNE 2003); P. 863–869, 8 FIGS., 1 TABLE.
10.1190/1.1581038

Tube-wave suppression in single-well seismic acquisition

Thomas M. Daley*, Roland Gritto*, Ernest L. Majer*, and Phillip West‡

ABSTRACT

Single-well seismic imaging is significantly hampered by the presence of borehole tube waves. A tube-wave suppressor has been tested using single-well seismic equipment at the Lost Hills (California) oil field. The suppressor uses a gas-filled bladder kept slightly above borehole fluid pressure. Field tests show a measurable reduction in tube-wave energy as compared to body waves propagating in the surrounding reservoir rock. When using a high-frequency (500–4000 Hz) piezoelectric source, the P-wave–tube-wave amplitude ratio was increased by 33 dB. When using a lower frequency (50–350 Hz) orbital vibrator source, the S-wave–tube-wave amplitude ratio was increased by 21 dB while the P-wave–tube-wave amplitude ratio was increased by 23 dB. These reductions in tube-wave amplitudes significantly improve single-well data quality.

INTRODUCTION

Single-well seismic data provide a scale of investigation which is intermediate between sonic log data and crosswell seismic data. In single-well seismic acquisition a seismic source and seismic sensors with designs appropriate for crosswell surveys are placed in the same borehole. In recent years, the single-well seismic technique has been investigated as a means to extend the resolution of well logging and as a means to provide imaging capability in areas not easily accessible with conventional crosswell or vertical seismic profiling (VSP), e.g., salt flank imaging.

An inherent and significant problem for single-well seismic surveys is borehole tube waves, as shown in numerical models (Kurkjian et al., 1994; Coates, 1998). One of the detrimental effects modeled and observed is the masking of body-wave reflections by the tube wave. Single-well seismic field experiments have been conducted by Lawrence Berkeley National Laboratory (LBNL) to develop and improve single-well seismic methodology (Majer et al., 1997; Daley et al. 2000a); however, the tube wave remains a significant problem. The results in this paper demonstrate the successful implementation of a tube-wave suppressor in a single-well survey.

Tube waves propagate in a fluid-filled borehole with amplitudes often much larger than body waves in the surrounding rock. A tube wave is an interface wave for a cylindrical interface between two media, typically a borehole fluid and surrounding elastic rock. Borehole waves, described by Lamb (1898), were observed in the early twentieth century (Sharpe, 1942; Ording and Redding, 1953) as summarized by White (1965). Using trapped (or guided) mode analysis, the classic tube wave can be seen as the lowest order trapped mode (Schoenberg et al., 1981). Higher order modes may be generated depending on material properties and source frequency. While the fundamental mode is usually called a Stoneley wave, the term Scholte wave is perhaps more appropriate for a solid–liquid interface.

Throughout many years of borehole seismology development, tube waves have most often been considered a problematic source of noise for those trying to measure material properties in the medium surrounding the borehole (Pham et al., 1993; Herman et al., 2000). Some work has been done to analyze tube-wave attributes to estimate rock properties (for example, Cheng et al. 1987; Kostek et al. 1998). This analysis, when successful, is limited to near-borehole information because tube-wave amplitude decays quickly with increasing distance from the fluid–rock interface. While single-well data present an opportunity for large-scale tube-wave logging, our work is focused on imaging features away from the borehole; therefore, the tube wave is considered noise. We present a description of the tube-wave suppressor designed at Idaho National Engineering and Environmental Laboratory (INEEL), followed by a description of field tests at the Lost Hills, California oil field and an analysis of the field tests which quantifies the reduction in tube-wave–body-wave amplitude ratio.

Manuscript received by the Editor March 21, 2002; revised manuscript received November 22, 2002.
*Lawrence Berkeley National Laboratory, Center for Computational Seismology, 1 Cyclotron Road, M.S. 90-1116, Berkeley, California 94720. E-mail: tmdaley@lbl.gov; rgritto@lbl.gov.
‡Idaho National Engineering and Environmental Laboratory, P.O. Box 1625, Idaho Falls, Idaho 83415.

TUBE-WAVE SUPPRESSOR DESIGN

Since the late 1990s INEEL has been working with LBNL to develop and deploy a tube-wave suppressor (TWS) specifically for use in single-well seismic surveys (West et al., 2002). The design uses a polymer bladder inflated to a pressure slightly higher than ambient borehole pressure. For field operation, a chamber is initially pressurized using gas (nitrogen) prior to deployment. Once the bladder is in the borehole fluid, a regulator maintains the volume of the bladder with nitrogen at pressure slightly more than ambient. We believe that the bladder provides pressure wave attenuation and energy dissipation. This implies that the bladder, which is exposed to the borehole fluid through perforations in the surrounding steel chamber, causes attenuation by converting tube-wave energy into heat as the compressional component of the tube wave excites oscillations of the gas in the bladder. When the suppressor is deployed to depths where borehole pressure exceeds the storage chamber's internal pressure, a valve opens, allowing the storage chamber's gas to be compressed by the borehole fluid and thereby maintaining bladder pressure. This borehole fluid pressurization allows operation at depths with pressure greater than the 2000 psi (1.4×10^7 Pa) chamber initial pressure (equal to about 1300 m in water).

A more detailed description of the INEEL TWS has three major components, shown schematically in Figure 1: (1) pressure chamber with lower excess flow valve, (2) wire feed-through, and (3) bladder chamber containing the bladder and pressure control system. The pressure chamber is a 0.08-m-diameter stainless steel pipe approximately 1.8 m long. It has been designed and tested per American Society of Mechanical Engineers requirements (ASME, 1998) for a pressure rating of 2000 psi (1.4×10^7 Pa). The chamber includes, on its top, a safety relief valve and an outlet port (to a regulator); on its bottom it has an input fill valve and an excess flow valve. The excess flow valve is configured to retain gas pressure internally to the chamber but to open when the borehole fluid pressure is greater than the gas pressure, allowing equalization to borehole pressure by intaking borehole fluid. The wire feed-through is comprised of a heavy-wall 0.025-m-diameter tube with O-ring surfaces on each end. The feed-through accepts connectors configured for multiple sensors (currently 56 wire maximum for 22-gauge wire). The pressure regulation system contained within the bladder chamber is a fail-open (i.e., release gas on failure), dual-stage assembly with excess pressure release valves. The system is based on a scuba diving regulator system but is reconfigured for extended depth. The second stage is extremely sensitive and can provide gas flow control over a range of a few inches of water pressure. The assembled system also includes ascent pressure control valving (to dump excess pressure to the borehole). The bladder is a soft polymer cylinder attached to the regulator outlet. The bladder and the regulator are contained within a perforated steel chamber for protection.

Figure 1 shows the INEEL TWS. The first deployment of the current design as part of LBNL's single-well system was in 1998 at a Baker-Atlas test well in Houston, Texas; however, the result was inconclusive (Daley et al. 2000a). In early 2001, the TWS was field tested with successful suppression of tube waves in shallow (100-m) wells at the University of California's Richmond Field Station (RFS) (Daley and Gritto, 2001). In those tests, tube-wave attenuation of 9 to 11 dB was measured with respect to body-wave amplitudes. Following the success of the RFS tests, further tests were conducted to measure the effectiveness in deeper wells with higher fluid pressures and faster rock velocities. These tests were conducted at Chevron's Lost Hills oil field in California as part of LBNL's single-well and crosswell seismic field experiments at a CO_2 injection site.

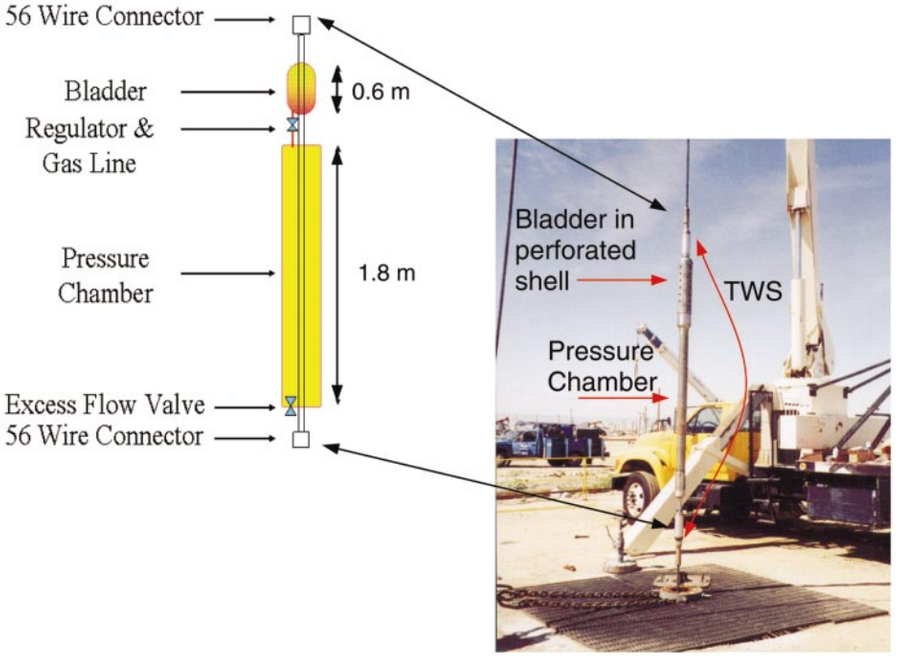

FIG. 1. INEEL tube-wave suppressor (TWS) in schematic (left) and as deployed at Lost Hills (right) as part of LBNL's single-well seismic equipment.

FIELD TESTS

The Lost Hills site is a producing oil field undergoing enhanced oil recovery as a pilot CO_2 injection project. (Figure 2). Observation wells were specifically drilled to allow geophysical monitoring of the CO_2 injection. Well OB-C1 was used as part of combined crosswell and single-well seismic surveys (Daley et al. 2000b; Gritto et al. 2002) as well as the TWS testing described here. The well was cased with 7-inch (0.18-m) fiberglass casing with an inside diameter (ID) of 6-inches (0.15 m), hung from $9\frac{5}{8}$-inch (0.24-m) steel surface casing at about 300 m depth. The well was water filled with small amounts of leaked hydrocarbons in the fluid. Table 1 has the material properties of the casing and borehole fluid as well as P- and S-wave velocities obtained from single-well and crosswell data acquisition at the site.

For single-well data acquisition, the TWS was placed in LBNL's single-well equipment string between the source and sensors (Figure 3). Two tests were analyzed for changes in tube-wave–body-wave ratio: one with a high-frequency piezoelectric source and one with a lower frequency orbital vibrator source (Daley and Cox, 2001). These tests are discussed individually following a discussion of tube-wave identification at the Lost Hills site.

Tube-wave identification

Analysis of field tests requires identification of the tube waves, which typically are identified by one or more of the following characteristics: large amplitude (relative to body waves), reverberant waveform, elliptical particle motion, and/or velocity (which is generally slower than body waves). In our field example we identify the tube waves by their velocity, which is intermediate between the formation P- and S-velocity. To ensure the identification of the tube wave, we solve for the expected velocity at the Lost Hills field site. The following solution for the velocity of a tube wave in cased and uncased wells in an infinite solid (assuming the wavelength is long compared to the borehole radius) was developed by White (1965). For an uncased well the tube-wave velocity C_T is

$$C_T = \left[\rho\left(\frac{1}{K} + \frac{1}{\mu}\right)\right]^{-\frac{1}{2}}, \tag{1}$$

where ρ is fluid density, K is bulk modulus, and μ is the rock shear modulus. This velocity can also be expressed in terms of P- and S-wave velocities α and β, respectively, as follows (Balch and Lee, 1984):

$$C_T = \left(\frac{1}{\alpha_1^2} + \frac{\rho_1}{\rho_2\beta_2^2}\right)^{-\frac{1}{2}}, \tag{2}$$

where subscript 1 is for the borehole fluid and subscript 2 is for the surrounding rock. For a cased well, White (1965) gives the tube-wave velocity as

$$C_T = \left[\rho\left(\frac{1}{K} + \frac{1}{\mu + \left(\frac{Eh}{2b}\right)}\right)\right]^{-\frac{1}{2}}, \tag{3}$$

where E is the casing's Young's modulus, h is the casing wall thickness, and b is the borehole radius. It is notable that the cased-well tube-wave velocity is significantly faster than the open-hole tube-wave velocity for the same borehole.

Using equation (3) and the parameters in Table 1, we calculated the tube-wave velocity for the field test well to be

Table 1. Well OB-C1 material properties.

Fluid P-wave velocity (m/s)	1500
Fluid density (kg/m^3)	1000
Rock density (kg/m^3)	1600
Rock S-wave velocity (m/s)	800
Rock P-wave velocity (m/s)	1675
Casing wall thickness (m)	0.0125
Casing radius (m)	0.09
Casing Young's modulus (N/m^2)	1.0×10^{10}

FIG. 2. Oil fields of the southern San Joaquin Valley, California. Lost Hills is north-west of Bakersfield.

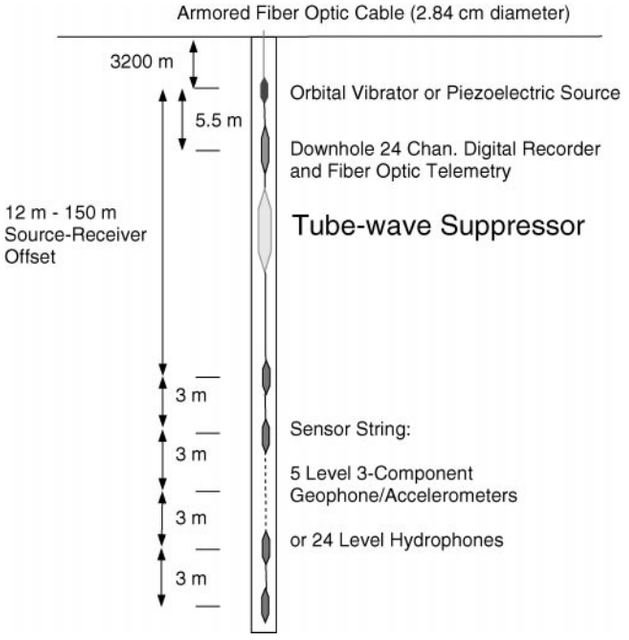

FIG. 3. Schematic of LBNL single-well seismic acquisition system with TWS.

987 m/s. The velocity of the seismic arrival, identified as a tube wave (Figure 4), varies from 975 to 1035 m/s. Thus, allowing for some variation in fluid and formation properties, the measured tube-wave velocities in our field test agree with the calculated velocity, confirming our identification of the tube wave.

Piezoelectric source test

The initial test used LBNL's piezoelectric source and hydrophone receivers for a single-well survey between 396 and 610 m at 0.6-m intervals. Unfortunately, after acquiring the single-well survey with the TWS, the hydrophone cable failed and a companion survey without the TWS could not be obtained. However, in previous work at this site, LBNL had obtained a single-well survey in the same well, covering the same depths, without the TWS. This previous work was part of a pre-CO_2 injection baseline survey. The only significant change was that different hydrophone sensors were used; therefore, absolute amplitudes cannot be compared. However, absolute amplitudes are unnecessary since our analysis uses amplitude ratios between body waves and tube waves. The same source and recording system was used in both surveys. Because the new sensor string had a longer lead-in cable and different sensor spacing, we limit our analysis to a sensor with the same source–receiver separation (offset). Using these data, the preinjection and postinjection single-well surveys form a data set to compare the piezoelectric source, hydrophone-sensor data recorded with and without TWS.

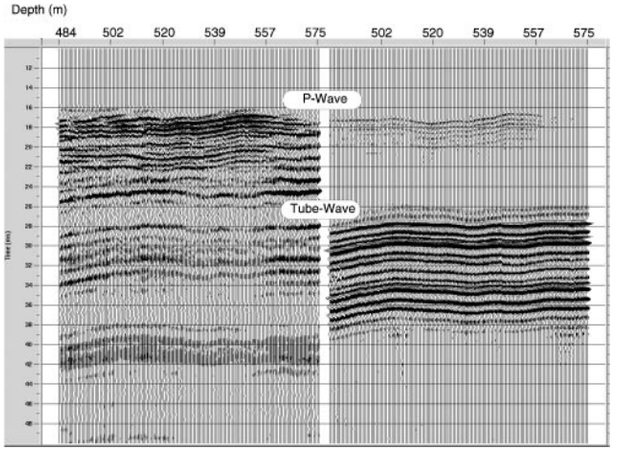

FIG. 4. Common offset gathers of single-well seismic data recorded with (left) and without (right) a TWS. The offsets are 27.4 m (left) and 27.1 m (right). Both data sets were acquired with a piezoelectric source and hydrophone receivers. Each trace is normalized by its own maximum amplitude. The reduction in tube-wave energy with respect to P-wave energy is easily visible.

Figure 4 shows the seismograms for a single-channel gather (equivalent to a common offset gather) for the two surveys. In the surveys with and without TWS, the source–receiver offset was 27.4 and 27.1 m, respectively. The qualitative reduction in tube-wave energy when using the TWS, as compared to P-wave energy, is clearly visible in the seismograms. To quantify the difference, we calculated the rms amplitude of an 11-sample (1.375-ms) moving window averaged for 16 representative traces and plotted this result in decibels (relative to the trace's maximum) as a function of time. This analysis, from the Paradigm Geotechnology Focus-3D commercial processing package, calculates the complex trace rms value $e(t)$ for a time window where $e(t) = \sqrt{[f(t)^2 + h(f(t))^2]}$ for recorded data $f(t)$ and where $h(f(t))$ is the Hilbert transform of the recorded data. Figure 5 shows this amplitude analysis for the data with and without TWS. The wave types (P-wave and tube wave) were identified using arrival time. The data recorded without TWS has a tube-wave amplitude 12 dB more than the P-wave amplitude. The data recorded with the TWS has a tube-wave amplitude 21 dB below the P-wave amplitude. The total increase in P-wave–tube-wave amplitude ratio is therefore 33 dB.

Orbital vibrator source test

A pair of tests were performed with and without the TWS using LBNL's orbital vibrator (OV) seismic source. In these tests, the data acquisition was repeated at the same time (post-CO_2 injection) with no change in equipment except for removing the TWS. The OV source generates circularly polarized waves which can be decomposed into two perpendicular, horizontal, linearly oscillating sources, i.e., x- and y-components of motion (Daley and Cox, 2001). Although this source has minimal volumetric change, and therefore should generate relatively low-amplitude tube waves, it has reportedly generated tube waves with amplitudes 20 dB greater than P-waves (Ziolkowski et al. 1999). In a single-well acquisition geometry, the OV is expected to generate S-waves as the largest vertically propagating body wave.

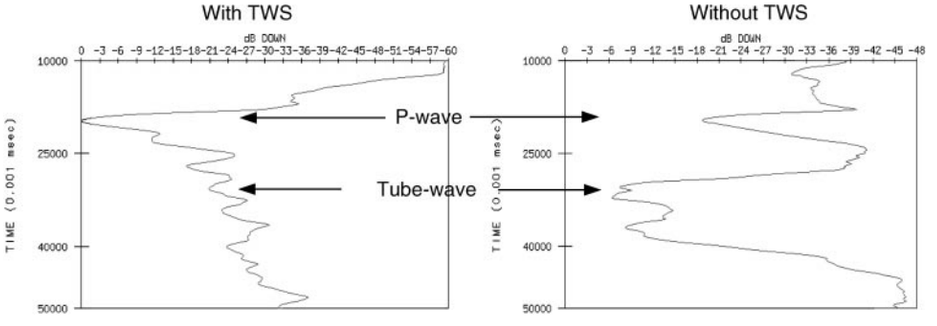

FIG. 5. Amplitude analysis of piezoelectric source single-well data recorded with (left) and without (right) the TWS. The amplitudes are rms in decibels down from the maximum for a moving window averaged over 16 traces. The data without TWS have a peak amplitude (0 dB) from source electrical crosstalk at zero time (not plotted). Comparison of the plots shows the TWS increases the ratio of P-wave to tube-wave rms amplitude by 33 dB (21 dB + 12 dB).

For the OV data acquisition we used a sensor string with three-component, wall-locking geophones. Therefore, this data set has six components of motion, two source components (x and y), and three sensor components (z, x, and y). These six-component data sets, with and without TWS, are shown in Figure 6 for one receiver gather (common offset of 26.2 and 26.8 m, respectively). A single geophone component of the data is shown in Figure 7. As with the piezoelectric source data, the OV data with TWS have a clear reduction in tube-wave energy compared to the same survey without TWS. Gain analysis was performed on the two OV data sets, again using an 11-sample window (2.75 ms) averaged for five representative traces from the y-component source and y-component sensor (shown in Figure 7). Figure 8 shows the results of this amplitude analysis for the OV data recorded with and without TWS. With the TWS, the shear wave has amplitude 16 dB greater than the tube wave; without the TWS, the shear wave is at least 5 dB lower in amplitude than the tube wave. The actual ratio may be greater because the highest amplitude in the shear-wave arrival time window for the case without TWS appears to be tube-wave multiples (see Figure 7). This is an inherent problem because the tube wave is faster than the shear wave in the Lost Hills diatomite. Nevertheless, we can obtain a lower bound for the amplitude ratio. The improvement in shear-wave–tube-wave amplitude ratio is at least 21 dB. The P-wave is relatively weak in the OV data (as expected for sensors vertically below a horizontally polarized source); however, a small peak is seen in the amplitude analysis of Figure 8 at the expected arrival time of a P-wave. The improvement in P-wave–tube-wave amplitude ratio associated with this peak is about 23 dB (+3 dB with TWS versus −20 dB without TWS).

CONCLUSIONS

The tube-wave suppressor designed and built by INEEL was successfully tested at oil-field scales with a single-well seismic acquisition system. In tests with a piezoelectric source and hydrophone sensors, the P-wave–tube-wave amplitude ratio was increased by 33 dB. In tests with an orbital vibrator source and wall-locking geophone sensors, the S-wave–tube-wave amplitude ratio was increased by 21 dB and the P-wave–tube-wave amplitude ratio was increased by 23 dB. These reductions are significant. In fact, the shear wave generated by the orbital vibrator source was only visible when using the TWS. The TWS design should allow operation at depths greater than those tested here and, in principle, allow simultaneous deployment of multiple TWS, which should further attenuate the tube wave.

We believe these results are sufficient to justify the use of the TWS in future single-well experiments. Furthermore, we expect that multiple TWS, or multiple bladders on one TWS,

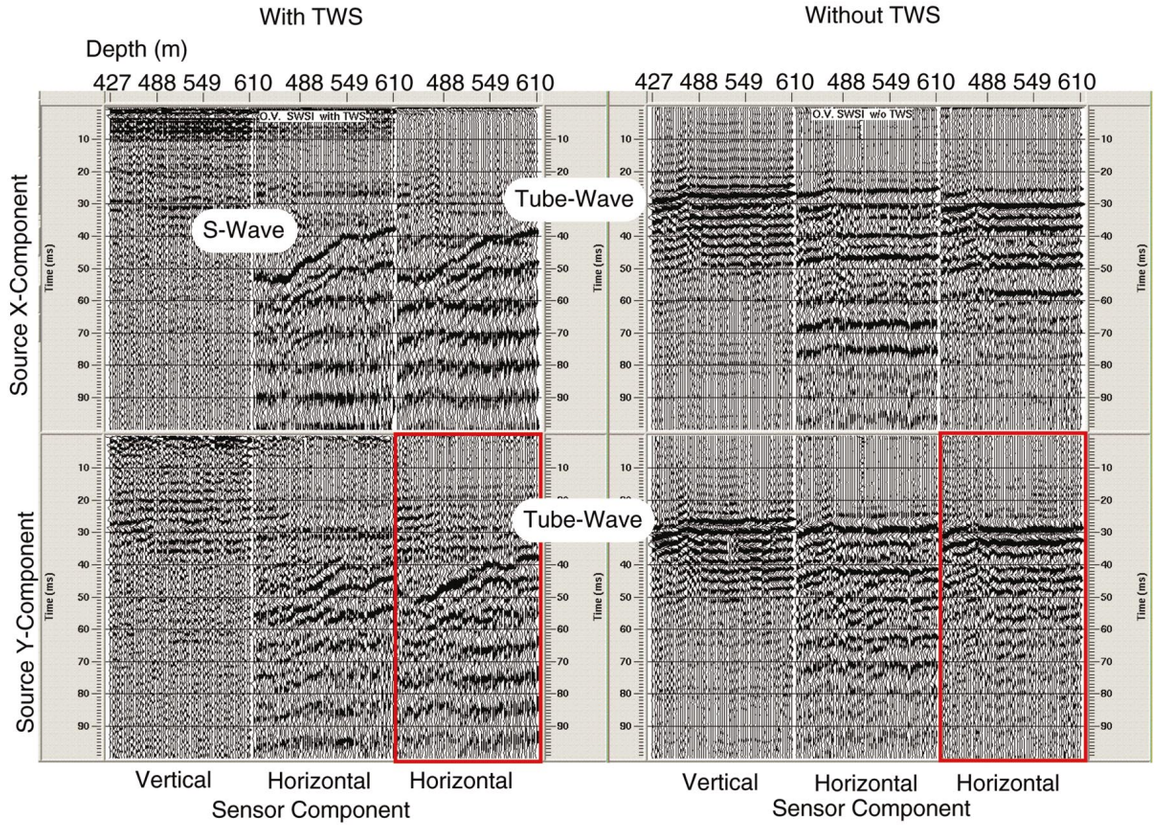

FIG. 6. Six-component single-well data acquired with the orbital vibrator source and three-component wall-locking geophone sensors. These data are a common offset gather with offset of 26.2 m with TWS (left) and 26.8 m without TWS (right). The top and bottom rows are the two source components (x and y) as measured by the three sensor components (z, x, and y). The data have been trace normalized (each trace normalized to its own maximum). The horizontal component data outlined in red were selected for analysis and are shown in Figure 7.

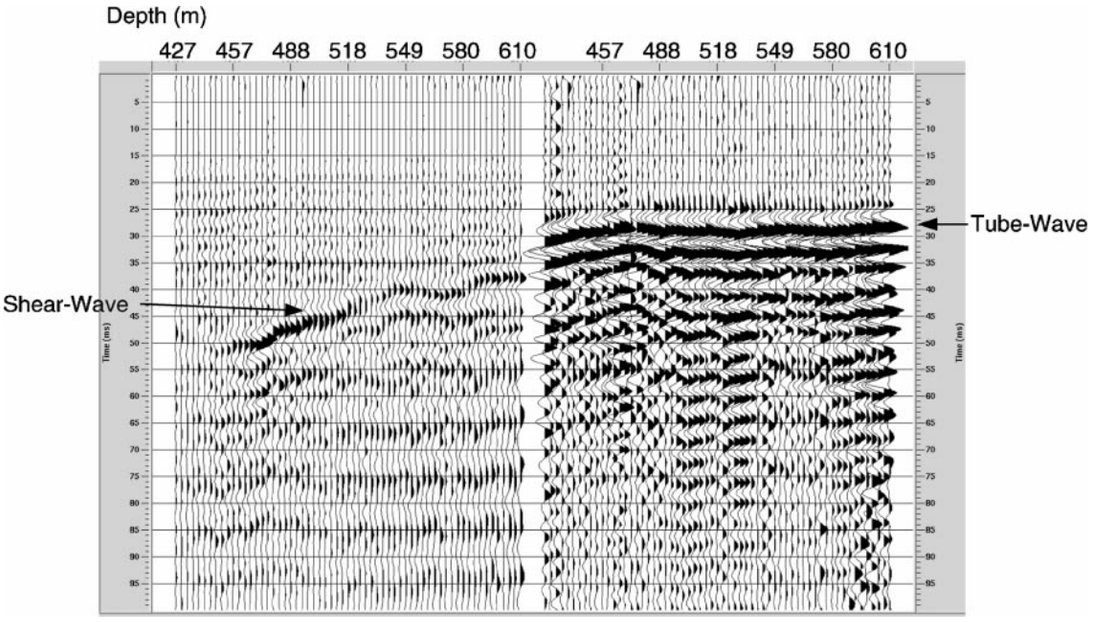

FIG. 7. Orbital vibrator source, single-well data in a common offset gather for a horizontal geophone with (left) and without (right) a TWS. Data are shown at true relative amplitude. The reduction in tube-wave energy when using the TWS is sufficient to allow identification of a shear-wave arrival (left), which is not identifiable in the data without a TWS (right).

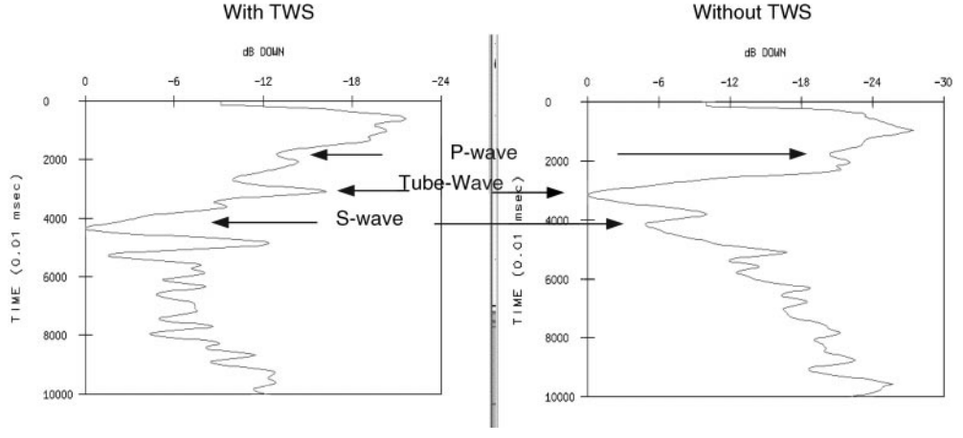

FIG. 8. An rms amplitude analysis of orbital vibrator source, single-well data recorded with (left) and without (right) a TWS. For the data recorded without a TWS, the tube wave is the largest arrival. In data recorded with the TWS, the S-wave is the largest amplitude arrival. Comparing the amplitudes at the S-wave arrival time, we observe a 21-dB improvement in S-wave–tube-wave amplitude ratio. The improvement in P-wave–tube-wave amplitude ratio is 23 dB.

would increase the tube-wave suppression. The results presented here demonstrate a method for improved seismic data quality in single-well experiments. It is likely that similar results can be obtained in crosswell, VSP, or other borehole seismic experiments.

ACKNOWLEDGMENTS

This work was supported by the Assistant Secretary for Fossil Energy, Office of Natural Gas and Petroleum Technology, the Natural Gas and Oil Technology Partnership program, of the U.S. Department of Energy under Contract DE-AC03-76SF00098. Data processing was performed at the Center for Computational Seismology, which is supported by the Director, Office of Science, Office of Basic Energy Sciences, Division of Engineering and Geosciences, of the U.S. Department of Energy under Contract DE-AC03-76SF00098. Thanks to Cecil Hoffpauir and Don Lippert of LBNL for help with single-well seismic imaging equipment development and data acquisition, Mike Morea of Chevron for support at Lost Hills field (and for providing Figure 2), and the members of the Single Well Seismic Imaging project.

REFERENCES

ASME, 1998, Boiler and pressure vessel code, VIII: Am. Soc. Mech. Eng.

Balch, A. H., and Lee, M. W., eds., 1984, Vertical seismic profiling: Technique, applications, and case histories: Internat. Human Res. Dev. Corp.

Cheng, C. H., Jinzhong, Z., and Burns, D. R., 1987, Effects of in-situ permeability on the propagation of Stoneley tube waves in a borehole: Geophysics, **52**, 1279–1289.
Coates, R. T., 1998, A modelling study of open-hole single-well seismic imaging: Geophys. Prosp., **46**, 153–175.
Daley, T. M., Majer, E. L., and Gritto, R., 2000a, Single well seismic imaging—Status Report: Lawrence Berkeley National Laboratory Report LBNL-45342.
Daley, T. M., Majer, E. L., Gritto, R., and Benson, S. M., 2000b, Borehole seismic monitoring of CO_2 injection in a diatomite reservoir: EOS, **81**, F272.
Daley, T. M., and Cox, D., 2001, Orbital vibrator seismic source for simultaneous P- and S-wave crosswell acquisition: Geophysics, **66**, 1471–1480.
Daley, T. M., and Gritto, R., 2001, Field tests of INEEL tube-wave suppressor and LBNL borehole seismic system at richmond field Station, February 2001: Lawrence Berkeley National Laboratory Report LBNL-49015.
Gritto, R., Daley, T. M., and Myer, L. R., 2002, Joint cross well and single well studies at Lost Hills, California: Lawrence Berkeley National Laboratory Report LBNL-50651.
Herman, G. C., Milligan, P. A., Dong, Q., and Rector, J. W., III, 2000, Analysis and removal of multiply scattered tube waves: Geophysics, **65**, 745–754.
Kostek, S., Johnson, D. L., and Randall, C. J., 1998, The interaction of tube waves with borehole fractures, part I: Numerical models: Geophysics, **63**, 800–808.
Kurkjian, A. L., Coates, R. T., White, J. E., and Schmidt, H., 1994, Finite-difference and frequency–wavenumber modeling of seismic monopole sources and receivers in fluid-filled boreholes: Geophysics, **59**, 1053–1064.
Lamb, H., 1898, On the velocity of sound in a tube, as affected by the elasticity of the walls: Manchester Memoirs, **42**, 1–16.
Majer, E. L., Peterson, J. E., Daley, T. M., Kaelin, B., Myer, L., Queen, J., Peter D'Onfro, and Rizer, W., 1997, Fracture detection using crosswell and single well surveys: Geophysics, **62**, 495–504.
Ording, J. R., and Redding, V. L., 1953, Sound waves observed in mud-filled well after surface dynamite charges: J. Acoust. Soc. Am., **25**, 719–726.
Pham, L. D., Krohn, C. E., Chen, S. T., and Murray, T. J., 1993, A tube wave suppression device for crosswell applications: 63rd Ann. Internat. Mtg., Soc. Expl. Geophys., Expanded Abstracts, 17–20.
Schoenberg, M., Marzetta, T., Aron, J., and Porter, R. P., 1981, Space-time dependence of acoustic waves in a borehole: J. Acoust. Soc. Am., **70**, 1496–1507.
Sharpe, J. A., 1942, The production of elastic waves by explosion pressures, II: Results of observations near an exploding charge: Geophysics, **7**, 311–321.
West, P. B., Weinberg, D. M., and Fincke, J. R., 2002, Empirical study of tube wave suppression for single well seismic imaging: Idaho National Engineering and Environmental Laboratory Report, INEEL/EXT-02-00274, Idaho Falls, Idaho.
White, J. E., 1965, Seismic waves: Radiation, transmission, and attenuation: McGraw-Hill Book Co.
Ziolkowksi, A., Sneddon, Z., and Walter, L., 1999, Determination of tube-wave to body-wave ratio for Conoco borehole orbital source: 69th Ann. Internat. Mtg, Soc. Expl. Geophys., Expanded Abstracts, 156–159.